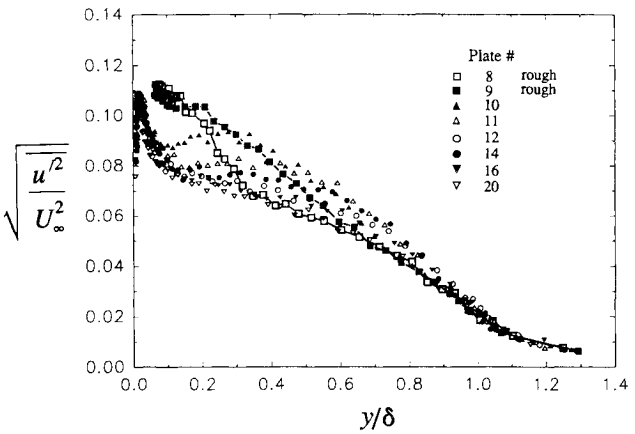


**Fig. 4 Turbulence intensity profiles over and downstream of the rough strip for $U_\infty$ = 12 m/s.**

each of the two rough plates and over selected smooth plates downstream of the roughness. The velocity profiles over the rough plates are indicated by the open and filled square symbols. These symbols are connected with line segments to aid in finding these profiles. The influence of the roughness is seen to be large. The velocity profile over the first rough plate (no. 8) is strongly retarded in the lower portion of the boundary layer relative to the smooth-wall profiles. The roughness influence extends to approximately $y/\delta$ = 0.4 where $\delta$ is the 99% boundary-layer thickness. Over the second rough plate (no. 9), the roughness influenced region extends to approximately $y/\delta$ = 0.7. Downstream of the roughness the velocity profiles quickly take on smooth-wall like characteristics near the wall, but an intermediate roughness influenced region is still apparent downstream of the interface.

Figure 4 shows the turbulence intensity, $\sqrt{\overline{u'^2}/U_\infty^2}$, profiles for the same conditions as the mean velocity profiles in Fig. 3. The evolution of the turbulent boundary layer is shown more clearly by this plot. Over plate no. 8 the near-wall turbulence intensity is much larger than equivalent smooth-wall conditions. The roughness influence clearly extends to about $y/\delta$ = 0.4. Over the other rough plate (plate no. 9) there is no additional increase in turbulence intensity very near the wall; however, the roughness influenced region extends much farther into the boundary layer to about $y/\delta$ = 0.7. After the roughness the turbulence intensity quickly takes on smooth-wall characteristics very near the wall. In the intermediate region the roughness influence continues to spread but decreases in magnitude. Downstream of the roughness there are three easily identifiable layers. Far from the wall the turbulent boundary layer continues to evolve as a smooth-wall boundary layer. In the intermediate region there is a roughness influenced internal layer. Very near the wall there is a smooth-wall-dominated internal layer which spreads to eventually envelop the entire layer. After some distance these three layers mix together to form a new smooth-wall boundary layer.

## Acknowledgment

The expert assistance of Mike West in the conduct of these experiments is gratefully acknowledged.

## References

[1]Taylor, R. P., "Surface Roughness Measurements on Gas Turbine Blades," *J. Turbomachinery*, Vol. 112, No. 2, 1990, pp. 175–180.

[2]Smits, A. J., and Wood, D. H., "The Response of Turbulent Boundary Layers to Sudden Perturbations," *Annual Review of Fluid Mechanics*, Vol. 17, edited by M. Van Dyke, J. V. Wehausen, and J. L. Lumley, Annual Reviews, Palo Alto, CA, 1985, pp. 321–358.

[3]Andreopoulos, J., and Wood, D. H., "The Response of a Turbulent Boundary Layer to a Short Length of Surface Roughness," *Journal of Fluid Mechanics*, Vol. 118, May, 1982, pp. 143–164.

[4]Taylor, R. P., Taylor, J. K., Hosni, M. H., and Coleman, H. W., Heat Transfer in the Turbulent Boundary Layer with a Step Change in Surface Roughness, American Society of Mechanical Engineers Paper 91-GT-266, 1991.

[5]Taylor, J. K., Taylor, R. P., Hosni, M. H., and Coleman, H. W., "An investigation of the Influence of a Step Change in Surface Roughness on Turbulent Flow and Heat Transfer," Mech. and Nuc. Eng. Dept., Mississippi State Univ., Rept. TFD-91-1, Mississippi State, MS, 1991.

[6]Coleman, H. W., Hosni, M. H., Taylor, R. P., and Brown, G. B., "Smooth Wall Qualification of a Turbulent Heat Transfer Test Facility," Mech. and Nuc. Eng. Dept., Mississippi State Univ., Rept. TFD-88-2, Mississippi State, MS, 1988.

[7]Coleman, H. W., Hosni, M. H., Taylor, R. P., and Brown, G. B., "Using Uncertainty Analysis in Debugging and Qualification of a Turbulent Heat Transfer Test Facility," *Experimental Thermal and Fluid Science*, Vol. 4, No. 6, 1991, pp. 673–683.

[8]Taylor, R. P., and Chakroun, W. M., "Heat Transfer in the Turbulent Boundary Layer with a Short Strip of Surface Roughness," AIAA Paper 92-0249, 1992.

[9]Hosni, M. H., Coleman, H. W., and Taylor, R. P., "Measurements and Calculations of Rough-Wall Heat Transfer in the Turbulent Boundary Layer, *International Journal of Heat Mass Transfer*, Vol. 34, Nos. 4 and 5, 1991, pp. 1067–1082.

# Determination of the Thermal Conductivity of Iron Aluminide as a Function of Temperature

Rick D. Wilson*
*U.S. Bureau of Mines, Abany, Oregon 97321*
and
Jack H. Devletian†
*Oregon Graduate Institute of Science and Technology, Beaverton, Oregon 97006*

## Introduction

THE thermal conductivity of several iron aluminide alloys was determined as a function of temperature. Four-point electrical resistivity data were used in conjunction with the Wiedemann-Franz-Lorenz equation[1] to determine the thermal conductivity of $Fe_3Al$. Rectangular sample bars were brought into equilibrium at several temperatures up to 1473 K before electrical resistivity measurements were made. A sample of iron with identical configuration, along with literature data, was used to verify the accuracy of the method. The results indicate that the thermal conductivity of $Fe_3Al$ alloys is independent of composition and increases linearly as a function of temperature.

One of the principal requirements for a heat transfer model is the accuracy of the values for the thermal conductivity as a function of temperature. Unfortunately, values for intermetallic iron aluminide alloys near the $Fe_3Al$ stoichiometric composition are unavailable in the literature.

Thus, the objective of this research was to determine the thermal conductivities of near-$Fe_3Al$ alloys over a wide range

Received Feb. 10, 1992, revision received May 11, 1992; accepted for publication May 12, 1992. This paper is declared a work of the U.S. Government and is not subject to copyright protection in the United States.

*Materials Engineer, 1450 SW Queen Avenue.
†Professor of Materials Science and Engineering, 19600 NW von Neumann Drive.

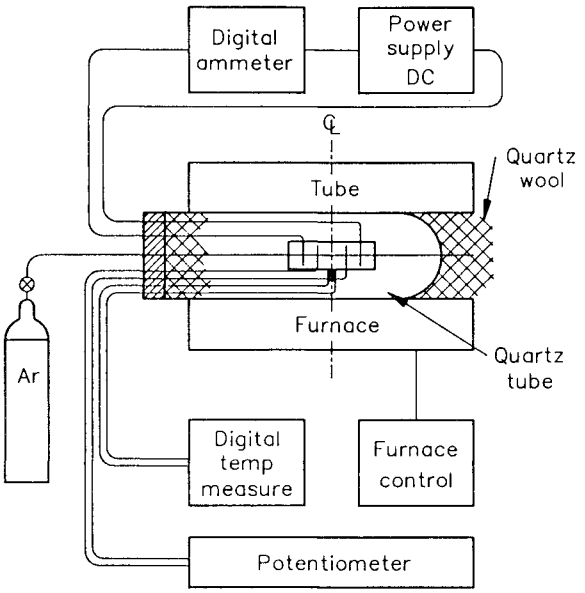


**Fig. 1 Electrical resistivity measurement apparatus equipment diagram.**

of temperatures. The three specific alloys investigated in this study included were 1) $Fe_{77}Al_{23}$, 2) $Fe_{73}Al_{27}$, and 3) $Fe_{76}Al_{24}$.

In metals and alloys, the electronic contribution to the thermal conductivity dominates thermal transport behavior. Particularly at elevated temperatures, thermal conductivity is related to temperature and electrical resistivity by the Wiedemann-Franz-Lorenz equation.[1] Slight differences in the composition of iron aluminide result in dramatic changes in the crystal structure and mechanical properties due to changes in the degree of B2 and $DO_3$ long range order associated with $Fe_3Al$.

## Materials and Procedures

Electrical resistance measurements were made using a four-point technique as described by Sutton.[2] Samples of electrolytic iron (for reference) and each of the three iron aluminide alloys, $Fe_{77}Al_{23}$, $Fe_{73}Al_{27}$, and $Fe_{76}Al_{24}$, were cut from vacuum induction melted castings. Each sample was 50-mm long, 5.5-mm wide, and 3.2-mm thick. Two type K thermocouple wires, 0.812-mm in diameter, were spot-welded perpendicular to each end of the sample. These wires were connected in series to a dc power supply and a digital ammeter as shown in Fig. 1. Between these wires, two 0.307-mm wires were also welded perpendicular to the sample and connected to a potentiometer. Since the exact distance between the wires must be known in order to precisely determine electrical resistivity, the distance was carefully measured, within $\pm 0.0025$ mm.

In turn, each sample was placed in a 25.4-mm i.d. quartz tube fitted with feed-throughs for argon gas flow, electrical wires, and a thermocouple. The quartz tube, sample, and thermocouple were located on the centerline in a tube furnace equipped with a differential temperature controller. A 1.0 $cm^3$/min flow of argon gas was used to prevent oxidation of the surface of the samples during heating. Each sample was heated and allowed to equilibrate at several temperatures ranging from 25 to 1100°C. The voltage was recorded at each temperature using several current settings to be sure a linear current/voltage relationship was obtained. The temperature profile down the length of the tube furnace was monitored to ensure a uniform temperature distribution over the length of the sample.

## Results and Discussion

Thermal conductivity values were measured experimentally at different temperatures up to 1100°C. For each test temperature, the applied voltage and current readings were found

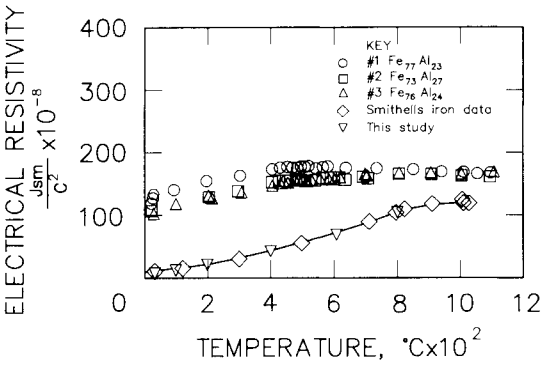


**Fig. 2 Electrical resistivity as a function of temperature for iron and iron aluminides.**

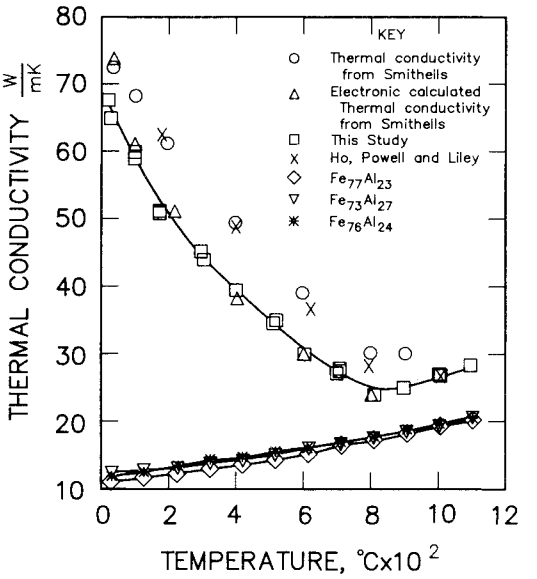


**Fig. 3 Thermal conductivity as a function of temperature for iron and iron aluminides.**

to increase linearly. As a result, the resistance values were simply the slope of the voltage-current curves for a particular temperature. The electrical resistivity could then be calculated by Eq. (1)

$$\rho = RA/L \tag{1}$$

where

$\rho$ = electrical resistivity, $Jsm/c^2$
$R$ = sample resistance of the test material, $Js/c^2$
$A$ = sample cross-sectional area, $m^2$
$L$ = distance between the wires connected to the potentiometer, m

The electrical resistivity for iron and each iron-aluminum alloy was plotted as a function of temperature and is shown in Fig. 2. Electrical resistivity of both the iron and $Fe_3Al$ alloys steadily increased as the temperature increased. However, values for the iron aluminides were an order of magnitude higher. Compositional differences had little effect on electrical resistivity as a function of temperature up to 1100°C as shown in Fig. 3. The Wiedemann-Franz-Lorenz equation[1] was used to calculate the electronic contribution to the thermal conductivity ($Ke$) for iron and each iron aluminide sample as described by Rossiter[3]

$$Ke = L \cdot Lo \cdot T/(R \cdot A) \tag{2}$$

where

$Lo = 2.443 \times 10^{-8} v^2 k^{-2}$ the Lorenz constant
$T$ = temperature in Kelvin

The experimental results for iron shown in Fig. 3 illustrate the characteristic decrease in thermal conductivity with increasing temperature, typical of an electrical conductor. On the other hand, the iron aluminides act more like insulators and show increased thermal conductivity as a function of temperature. At lower temperatures the electrical conductivity of iron aluminide has an electrical conductivity between metals with $10^{23}/cm^3$ conduction electrons and semimetals like As with $10^{21}/cm^3$. However, the thermal conductivity of iron and iron aluminide is only an order of magnitude apart, whereas, for insulators like sulfur with $10^{13}/cm^3$ conduction electrons, it is 10 orders of magnitude lower in electrical conductivity than iron aluminide. This results from an increase in the number of conducting electrons available for energy transfer at the higher temperatures. Figure 3 indicates that compositional differences near stoichiometric $Fe_3Al$ have little effect on the thermal conductivity as a function of temperature.

The accuracy in the thermal conductivity determination depends on the accuracy of the temperature as well as the accuracy and stability of the voltage and current measurements. Electrical resistance and thermal conductivity data for iron showed Curie transformations at 1043 K.[4] Similar results were reported by Smithells.[5] The temperature control was $\pm 1$°C, and the temperature profile was reasonably uniform. Accuracy of the experimental resistance measurements was $10^{-4}/cm^2$.

Unfortunately, this sensitivity is inadequate to detect the order/disorder transitions in iron aluminide. The samples were 50-mm iron aluminide rectangular bars with a 10-to-1 aspect ratio. According to Vennegues et al.[6] an aspect ratio greater than 100-to-1 is necessary to observe the resistivity changes due to the order/disorder transformations. Larger temperature steps are also necessary due to the strong magnetic effects associated with spin disorder scattering and electronic structure effects. Nevertheless, the experimental results are consistent with the recommended iron thermal conductivity data from Ho et al.[4] shown in Fig. 3. They compiled 75 papers reporting iron thermal conductivity data.

## Conclusions

1) Compositional differences had little effect on the thermal conductivity of iron aluminide alloys in the region of $Fe_3Al$ ($Fe_{77}Al_{23}$, $Fe_{73}Al_{27}$, and $Fe_{26}Al_{24}$).

2) Thermal conductivities of iron aluminide alloys in the region of $Fe_3Al$ increase linearly as a function of temperature.

3) Electrical resistivity measurements for iron used in thermal conductivity calculations are in agreement with available literature values.

## References

[1]Ashcroft, N. W., and Mermin, N. D., *Solid State Physics*, Holt, Rinehart and Winston, Philadelphia, PA, 1976, p. 22.

[2]Sutton, W. H., "Apparatus for Measuring Thermal Conductivity of Ceramic and Metallic Materials to 1200°C," *American Ceramic Society*, Vol. 43, No. 2, 1960, pp. 81–87.

[3]Rossiter, P. L., "Electrical Resistivity Near the Critical Point in Binary Alloys," *Journal of Physics F: Metal Physics*, Vol. 10, No. 7, 1980, pp. 1459–1465.

[4]Ho, C. Y., Powell, R. W., and Liley, P. E., "Thermal Conductivity of the Elements," *Journal of Physical Chemical Reference Data*, Vol. 3, Supp. 1, 1974, pp. 1:366–1:337.

[5]Smithells, C. J., *Metals Reference Book*, Interscience, New York, 1955, p. 636.

[6]Vennegues, P., Cadeville, C., Pierron-Bohnes, V., and Afyouni, M., "Strong Decrease of the Activation Energy as a Function of Al Content in $FeAl_x$ Alloys ($x \leq 30$ at .%) Deduced from Kinetic Measurements of Ordering," *Acta Metallurgica et Materilia*, Vol. 38, No. 11, 1990, pp. 2199–2213.

# Characterization of Thermal Performance of Fibrous Insulations Subject to a Humid Environment

K. Vafai*
*Ohio State University, Columbus, Ohio 43210*

## Nomenclature

$A$ = aspect ratio, $\bar{H}/\bar{L}$
$\bar{H}$ = height of the porous insulation, m
$\bar{H}'$ = length of the opening, m
$\bar{K}$ = permeability, $m^2$
$\bar{k}_i$ = thermal conductivity for phase $i$, W/m-K
$\bar{k}_{\text{eff}}$ = effective thermal conductivity, W/m-K
$\bar{L}$ = thickness of the insulation, m
$Le$ = Lewis number, $\bar{\alpha}_{\text{eff},0}/\bar{D}_{v,\text{eff}}$
$\dot{m}$ = condensation rate
$Pe$ = Peclet number, $\bar{v}_{\gamma,0}\bar{L}/\bar{\alpha}_{\text{eff},0}$
$T$ = dimensionless temperature, $\bar{T}/\Delta\bar{T}$
$\bar{T}_{\infty,c}$ = cool-side ambient temperature, K
$\bar{T}_{\infty,h}$ = hot-side ambient temperature, K
$\varepsilon$ = volume fraction
$\eta$ = opening size, $\bar{H}'/\bar{H}$
$\rho_i$ = dimensionless density for phase $i$, $\bar{\rho}_i/\bar{\rho}_{i,0}$
$\rho_v$ = dimensionless vapor density, $\bar{\rho}_v/\bar{\rho}_{v,0}$

*Subscripts*
$a$ = air phase
$c$ = cool side
eff = effective properties
$h$ = hot side
$i$ = $i$th phase
$s$ = saturation quantities
$v$ = vapor phase
$\beta$ = liquid phase
$\gamma$ = gas phase
$\sigma$ = solid matrix
$\infty$ = ambient
0 = reference quantities

*Superscript*
- = dimensional quantities

## Introduction

IN this work the insulating capability of a typical Fiberglas® insulation slab is evaluated when it is exposed to different types of environment on each side of the slab. The investigation is based on the theoretical work that takes heat conduction, natural convection, phase change, and gas infiltration into account. The results are analyzed and combined with the latest theoretical work and useful heat transfer characteristics are found for each of the materials studied. Various curves for the heat flux are obtained in which several pertinent parameters are varied and their effects on the heat transfer behavior are observed. These parameters include the humidity, temperature, and pressure differences across the insulation, the thickness of the insulation matrix, and the opening sizes and their respective locations. It is shown that the moisture within the material and the gas infiltration significantly

Received Sept. 3, 1991; revision received Feb. 28, 1992; accepted for publication March 2, 1992. 

*Professor of Mechanical Engineering, Department of Mechanical Engineering. Member AIAA.